# SEARCH FOR FINITE DIMENSIONAL ATTRACTORS IN ATMOSPHERIC TURBULENCE

RUDOLF O. WEBER, PETER TALKNER, GÉRARD STEFANICKI and LUC ARVISAIS*
*Paul Scherrer Institute, CH-5232 Villigen PSI, Switzerland*

**Abstract.** The question is investigated whether the dynamics of turbulent wind fields in the atmospheric boundary layer can be satisfactorily described by a low-dimensional deterministic system. Special emphasis is laid on the detection of a possibly existing, underlying strange attractor. Fast response wind measurements of an ultrasonic anemometer with a sampling rate of 21 Hz were carried out over periods of several days in the near surface boundary layer. The correlation dimension of the resulting time series, several million data points long, is estimated by means of the Grassberger–Procaccia algorithm. No sign of a low dimensional attractor can be detected. By comparison with different types of random noise, the existence of an attractor with dimension lower than six can be excluded in the present data sets.

## 1. Introduction

The seminal paper by Lorenz (1963) is one of the earliest works describing chaotic motions on a low-dimensional attractor. Chaotic motion is characterized by an intrinsic instability causing the system to be sensitive to initial conditions. As a consequence, trajectories from nearby initial points separate exponentially in phase space. At that time, it came as quite a surprise that a dynamical system with three degrees of freedom only, i.e. described by three ordinary differential equations of first order, could exhibit completely unpredictable motions. Since Lorenz (1963) employed his model as a crude approximation of the dynamics of a convective fluid layer, it was soon conjectured that also the atmosphere might have an intrinsic limit of predictability and it was even speculated that atmospheric dynamics might be governed by a low-dimensional attractor. Later, tools were developed by means of which the attractors of dynamical systems can be characterized (Hentschel and Procaccia, 1983). These concepts were generalized in order to test whether observed time series might have a deterministic origin and if so, to characterize the respective attractor by its possibly fractal dimension (Grassberger and Procaccia, 1983). Nicolis and Nicolis (1984) reported the existence of a climatic attractor from an isotope record of a deep-sea core extending over the last million years but their work was soon criticized (Grassberger, 1986). The main objection against the validity of the findings of Nicolis and Nicolis (1984) is the small number of data points they used in their analysis (Grassberger, 1986; Tsonis *et al.*, 1993). Many subsequent papers reported low-dimensional attractors of the climate system and of the atmosphere, some of which are mentioned below. Fraedrich (1986) claims the

* Permanent Affiliation: Waterloo University, Ontario, Canada.

existence both of a climate attractor with dimension 4.4, based on data from a deep-sea core covering the last 800,000 years, and of a weather attractor with dimension of about 3–4, estimated from daily meteorological elements. Based on other daily meteorological data sets, a weather attractor of dimension 5–6 was reported in Essex *et al.* (1987) and a weather attractor of dimension 7–8 in Keppenne and Nicolis (1989). Even for very short time scales, it was claimed that a low-dimensional attractor governs the dynamics of the atmosphere. In Tsonis and Elsner (1988), 10 s averages of wind measurements were analysed and a attractor dimension of 7.3 was found. In Poveda–Jaramillo and Puente (1993), wind and temperature data, sampled every 0.1 s, led the authors to the conclusion that a 4–6 dimensional attractor governs the short-term dynamics of the atmosphere. The discussion still continues whether a low-dimensional climatic attractor or weather attractor exists. Some of the results of different analyses and critiques are summarized by Ruelle (1990) and Tsonis (1992).

Among the physical arguments indicating the possibility of low-dimensional attractors in turbulence is the existence of large-scale structures that might act as rigid objects being describable by only a few degrees of freedom, as for example in Rayleigh–Bénard convection. However, the mathematical and physical understanding of fully developed turbulence as the high dimensional phenomenon *per se* (Temam, 1989), though yet incomplete, is at variance with the picture of low dimensional dynamics which can describe various aspects of so called weak turbulence (Manneville, 1990). The prominent scaling property of the power spectral density is traditionally modelled by means of hierarchical models with the number of levels increasing with the strength of the turbulence (Richardson, 1922; Kolmogorov, 1941).

Even if the dynamics of a physical system evolve chaotically on a low-dimensional attractor, it is still not guaranteed that this behaviour can be discovered from a finite set of values of a single observable of the system which is discretely sampled and measured with finite accuracy. One of the most severe restrictions to the estimation of an attractor dimension is the number of available data points (Smith, 1988; Ruelle, 1990; Nerenberg and Essex, 1990). Different and contradictory upper bounds to the attractor dimension that can be reliably estimated from a given number of observations were derived from theoretical reasoning. Without entering this controversy, we choose another way of finding limitations to the estimation of attractor dimensions. The primary question to be answered is whether the observed signal can be distinguished from random noise, which in principle has infinite dimension. Any numerical algorithm which estimates dimensions from time series can only handle a finite number of data. Therefore, pseudorandom noise of finite length will not yield an infinite dimension, but finite size effects reduce the observable dimension. As these finite size effects can hardly be analytically estimated, we perform numerical simulations to see their influence on the dimension estimates. We take therefore appropriate types of random noise of the same length, variance and number of digits as the observed time series and compare the

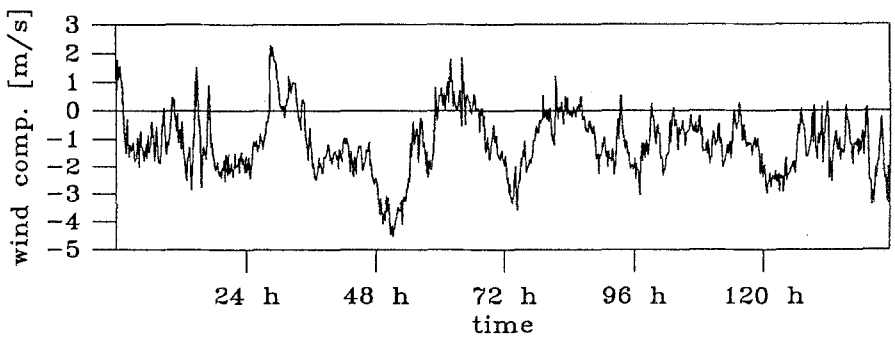


Fig. 1. Ten-minute averages of a horizontal wind component (in m/s) for the measurement period #1 as described in Table I. The time series starts on 15 January 1993 at 10:45 Central European time.

results of the corresponding dimension calculations for the observed time series with those for the random noise.

## 2. Wind Data

We measured wind fields in the atmosphere by means of an ultrasonic anemometer by Gill Instruments Limited. This type of instrument measures the flight time of ultrasonic pulses along a short path (about 15 cm) which allows one to determine the wind velocity along the path direction by means of the Doppler effect. As three crossed paths are used, the full three-dimensional wind vector can be reconstructed. Due to the geometry of the instrument, the vertical wind component is determined with much less accuracy than the horizontal components. Therefore, only one of the horizontal components of the wind vector is analyzed. The instrument was placed on top of a 10 m high mast on the roof of a three-storied building on the grounds of the Paul Scherrer Institute.

The sampling time of the anemometer is 0.048 s, corresponding to a sampling rate of about 21 Hz. Four periods, each five to six days long, were selected for dimension analyses. A summary of their characteristics is given in Table I. The time series of 10-min averages of the horizontal wind component for the first of the four selected periods is shown in Figure 1. A clear diurnal cycle of the horizontal wind component can be seen, indicating that the wind is thermally influenced. In the upper chart of Figure 2, the autocorrelation function of the first ten minutes of time series #1 is plotted. The first zero crossing occurs roughly after 1500 time steps (or 72 s). This zero crossing time depends strongly on the length of the interval used for computation of the autocorrelation function. The autocorrelation estimated from the whole time series is shown in the lower chart of Figure 2. The first zero crossing occurs after about 300,000 time steps (or 14,400 s). This discrepancy between the different zero crossing times is already an indication that there is no intrinsic time scale present in the dynamical system.

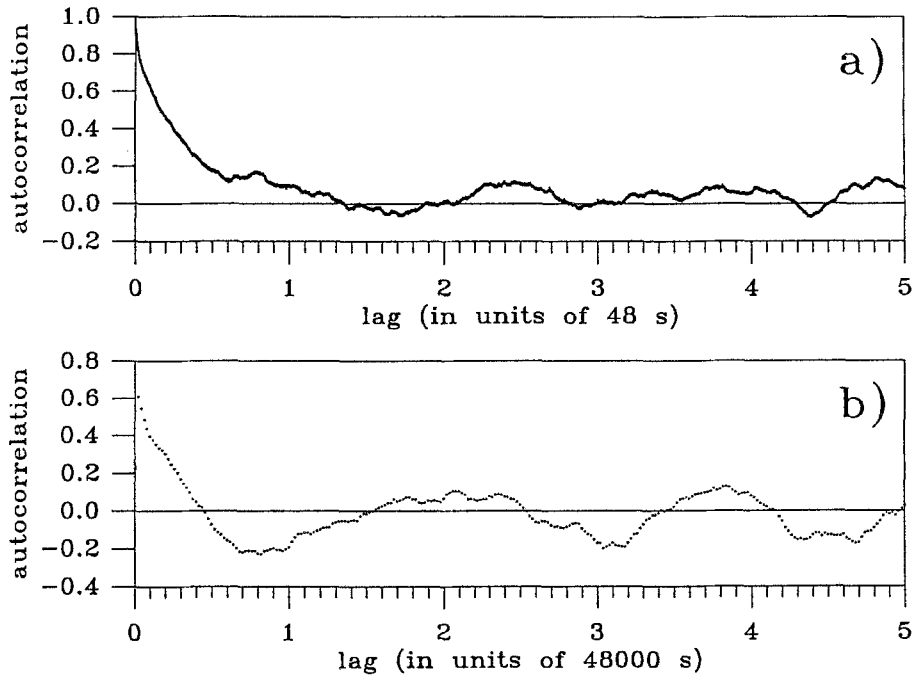


Fig. 2. (a) Autocorrelation function estimated from the first 10 min of time series #1. All lags from 0.048 s up to 240 s are shown, i.e., from 1 to 5000 in units of the sampling time of 0.048 s. (b) Autocorrelation of time series #1 estimated form the whole time series. Only lags that are multiples of 960 s are considered.

TABLE I

Specifications of the four selected observation periods

| Number | Starting date | Starting time (CET) | Length in hours | Number of data points | Standard deviation |
|---|---|---|---|---|---|
| #1 | 15 Jan. 1993 | 10:45 | 143 | 10,742,500 | 1.30 m/s |
| #2 | 05 Feb. 1993 | 16:25 | 141 | 10,580,000 | 0.83 m/s |
| #3 | 26 Mar. 1993 | 9:05 | 123 | 9,187,500 | 1.32 m/s |
| #4 | 05 Jan. 1993 | 15:35 | 137 | 10,270,000 | 1.44 m/s |

To shed further light on the nature of the observed time series of horizontal wind components, a power spectral analysis is performed. The observed time series are split up into segments of 16,384 data points (about 13 min). In each segment, the mean is subtracted, which automatically eliminates the diurnal cycle present in the time series. The power spectrum of each segment is computed by applying a Welch window to the data and a Fast Fourier transform (Press *et al.*, 1992). The power spectra of all segments are averaged in order to reduce the statistical error

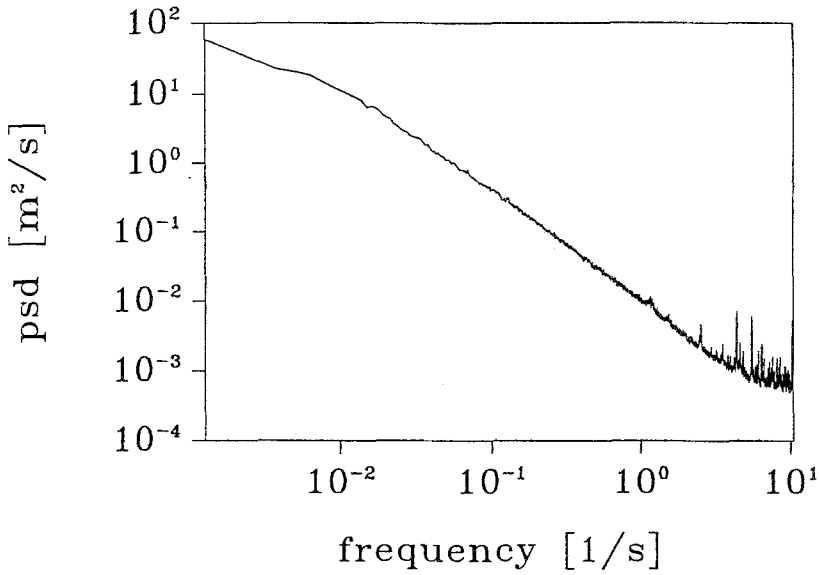


Fig. 3. Power spectral density (psd) of a horizontal wind component for observation period #1.

of the spectral estimate. In Figure 3 the power spectral density of time series #1 is shown. There is no clear peak in the spectrum, which shows again that there is no prevailing frequency in the time series. Over a wide range, the power spectral density has a scaling behaviour $\sim f^{-\alpha}$ with $\alpha = 1.54$. For the other three time series, the estimated $\alpha$ ranges from 1.53 to 1.58, which is somewhat below the 5/3 resulting from Kolmogorov's theory for isotropic and homogeneous turbulence (Kolmogorov, 1941).

## 3. Dimension Calculations

In general, an attractor can be described by an infinite set of dimensions, which may possibly take non-integer values (Hentschel and Procaccia, 1983). As most of them will indicate whether the system is low-dimensional or not, one can choose a dimension which is easy to compute for the analysis of some given data. As in many other analyses, we also choose the well discussed and analysed correlation dimension $D_2$.

The record of a single horizontal wind component constitutes a scalar time series. The first task in the dimension calculation is to embed the dynamics of the system in a multidimensional phase space, the embedding space (Mane, 1981; Takens, 1981). This is done by the method of delay coordinates (Takens, 1981; Grassberger and Procaccia, 1983). Given the scalar observations $x_i$ $(i = 1, \ldots, N)$,

a time series of vectors $\vec{v}_i$ $(i = 1, \ldots, N - (m-1)\tau)$ with $m$ components is constructed by $m$ consecutively following $\tau$-th neighbors:

$$\vec{v}_i = (x_i, x_{i+\tau}, x_{i+2\tau}, \ldots, x_{i+(m-1)\tau}), \tag{1}$$

where $\tau$ is the so-called delay time. The components of the vector are thus the time-delayed values of the scalar observations. The $m$ dimensional Euclidian space in which these vectors lie, forms an embedding space. If the time series is generated by the motion on an attractor of a finite dimensional dynamical system, the trajectory in the embedding space displays many of the properties of the original dynamics, provided the dimension of the embedding space is sufficiently large (Mane, 1981; Takens, 1981). Especially the dimension of the embedded attractor coincides with that of the true attractor.

No definite answer has yet been given to the question of which delay time is the right choice. For an infinite number of noise-free data points, there is no restriction for the delay time (Takens, 1981). Clearly, for a finite set of data, $\tau$ cannot be chosen arbitrarily large. On the other hand, a too small delay time introduces strong correlations of the components of the vectors $\vec{v}_i$. This may change the dimension estimate in an unpredictable manner. Often a scatterplot of $x_{t+\tau}$ against $x_t$ (return map) can help to choose a delay time. For many low-dimensional systems, the points in the return map are centered close to the diagonal for small delay times $\tau$, due to short-term correlations, and start to spread out with increasing delay time, indicating that the correlations decrease. The value of the delay time where this transition takes place gives a reasonable estimate of the delay time to be used in the embedding procedure. Return maps with different delay times ranging from 1 to 5000 were made for portions of the data sets. In Figure 4 two examples are shown with delay time 1 and 1000. Already for a delay time of 1, the points are not too close to the diagonal. For increasing values of the delay time, no clear transition as described above occurs. Return maps of the other time series give the same result, which confirms the conclusion that there is no characteristic correlation time scale in our measurements of atmospheric turbulence. Hence, the return maps do not reveal a characteristic delay time. Therefore, we choose the time of the first zero-crossing of the short-term autocorrelation function as delay time. To test the influence of the choice of delay time, the dimension calculations are carried out with different delay times as discussed below.

For a fixed embedding dimension, the time series of vectors $\vec{v}_i$ in the embedding space is used to calculate the so-called correlation integral proposed by Grassberger and Procaccia (1983):

$$C(r, N) = \frac{1}{N^2} \sum_{\substack{i,j=1 \\ i \neq j}} H(r - |\vec{v}_i - \vec{v}_j|), \tag{2}$$

where $H(x)$ is the Heavyside step function and $|\vec{y}|$ denotes a distance measure in the embedding space. Hereafter the Euclidian distance is always used. The

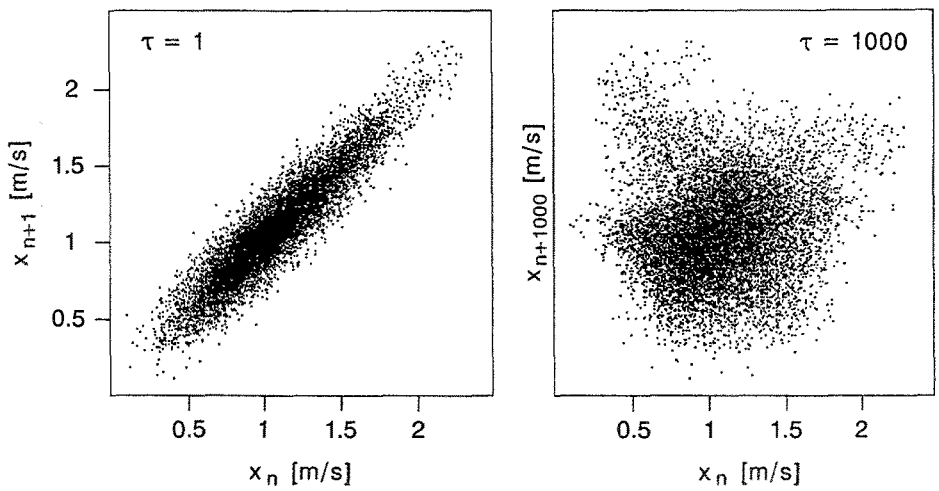


Fig. 4. Return map of a horizontal wind component for observation period #1. In the left chart, the delay time is 1; in the right chart the delay time is 1000.

correlation integral (2) counts the relative frequency of pairs whose separation is smaller than the scale $r$. The correlation dimension is then defined as

$$D_2 = \lim_{r \to 0} \lim_{N \to \infty} \frac{\log C(r, N)}{\log r}. \tag{3}$$

In practice for a finite set of data with discrete time resolution and finite accuracy, neither of the limits in (3) can rigorously be performed. But in a plot of $\log C(r, N)$ versus $\log r$, a linear part appears for intermediate values of $r$. Its slope is taken as an estimate of the correlation dimension. The range of this linear region can be enlarged by changing the original definition of the correlation integral (2) by considering only vectors which are at least $W$ time steps apart (Theiler, 1986),

$$C(r, N, W) = \frac{2}{N^2} \sum_{n=W}^{N} \sum_{i=1}^{N-n} H(r - |\vec{v}_{i+n} - \vec{v}_i|). \tag{4}$$

For $W = 0$, self-pairs are included, whereas $W = 1$ corresponds to the standard Grassberger–Procaccia algorithm. A discussion of the effect of inclusion of self-pairs is given in Smith (1988).

For numerical purposes, some additional modifications are made to the original Grassberger–Procaccia algorithm. First, not the full matrix of distances between all pairs of vectors in the embedding space is computed, but a set of $M$ reference points (some thousand) is selected for which the distances to all other points in the embedding space are determined. This still leads to good statistics and reduces the required computation time drastically. Furthermore, an additional free parameter is introduced in the construction of the vectors in the embedding space.

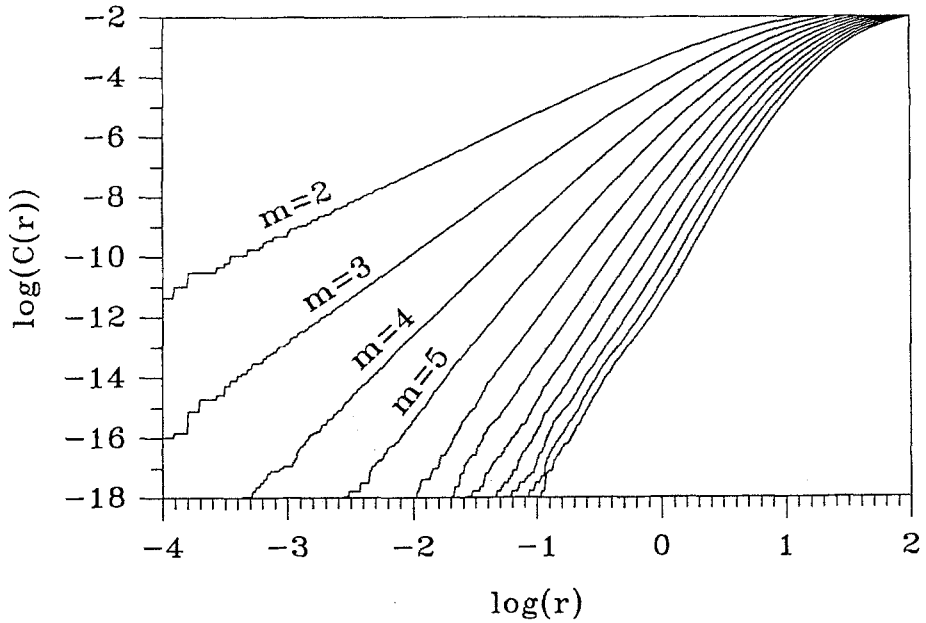


Fig. 5. Correlation integral as a function of linear scale $r$ for time series #1, where log denotes the natural logarithm. Different embedding dimensions are used and are labeled by $m$. The delay time is $\tau = 1500$.

Not each point in the embedding space is taken into account, but only points $a$ time steps apart are used, thus $\vec{v}_1 = (x_1, x_{1+\tau}, \ldots, x_{1+(m-1)\tau})$ and $\vec{v}_2 = (x_{1+a}, x_{1+a+\tau}, \ldots, x_{1+a+(m-1)\tau})$ and so on. A value of $a$ greater than one leads to a reduction of required computing time and can also improve the extension of the scaling range in the log $C(r, N)$ versus log $r$ plot.

Once the delay time is fixed, the correlation dimension of the system is calculated for different dimensions of the embedding space. The maximal embedding dimension is chosen in such a way that there is still a reasonable scaling range of the correlation integral as a function of size $r$. For the present data, we found 12 as a maximal embedding dimension. This is in good agreement with the theoretical estimate of 13 given in Nerenberg and Essex (1990).

In order to eliminate the diurnal cycle, the data are split into segments of one day length, corresponding to $1.8 \times 10^6$ data points. The correlation integrals are calculated for each one-day segment and then averaged. In Figure 5 a graph of the correlation integral versus the scale $r$ is shown for time series #1 with a delay time $\tau = 1500$ and different embedding dimensions. For each embedding dimension, a linear range shows up in an intermediate range of $r$.

In Figure 6, the resulting correlation dimension as a function of the embedding dimension is shown for all four time series of horizontal wind component. For none of the time series does the correlation dimension saturate with increasing embedding dimension, as one would expect for a time series stemming from a system

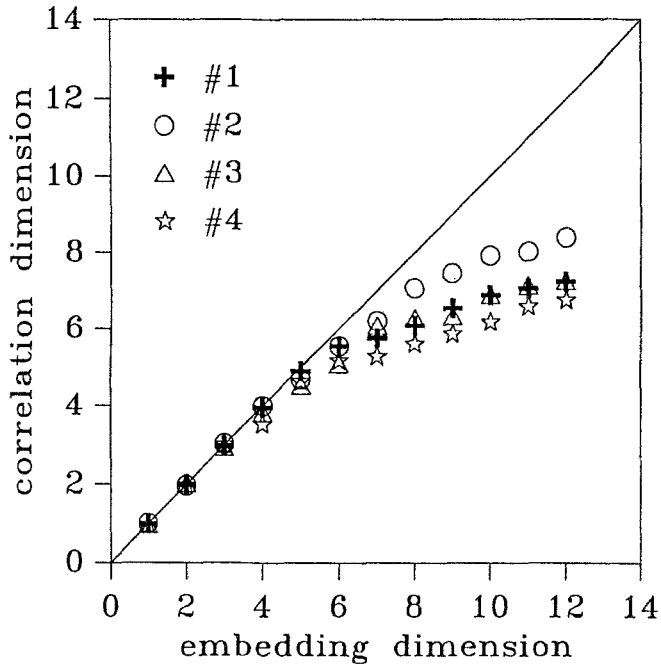


Fig. 6. Correlation dimension as a function of embedding dimension for the four time series of horizontal wind component.

with an underlying low-dimensional attractor; see also the next section. However, the results deviate quite strongly from the diagonal on which the correlation dimensions of infinitely long purely random time series would fall.

As neither the return maps nor the graphs of the autocorrelation function could unambiguously reveal a proper delay time, the dimension calculations are performed with different delay times. In Figure 7, the correlation dimension as a function of the embedding dimension is shown for time series #3 for different choices of delay time. However, for none of the delay times between 1 and 10,000 does the correlation dimension saturate with increasing embedding dimension.

## 4. Comparison with Random Noise

In order to see how much of the deviations of the correlation dimensions from the diagonal in Figure 6 is caused by the finite length and accuracy of the measurements, different kinds of random noise are generated which have the same length and accuracy as the observed data. These synthetic data are used as a null hypothesis in order to decide whether the observed data can be discriminated from stochastic data by means of a dimension analysis. Autoregressive processes of first order, $AR(1)$, and of second order, $AR(2)$, are generated (Priestley, 1981). They are described by

$$AR(1): \; x_n + a_1 x_{n-1} = \epsilon_n, \tag{5}$$

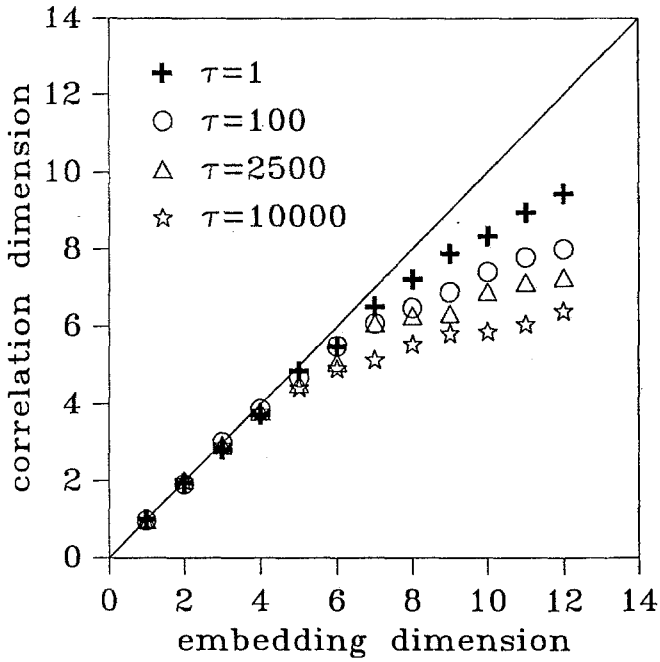


Fig. 7. Same as Figure 6, but for the observation period #3 with different delay times $\tau$.

$$AR(2): \; x_n + \alpha_1 x_{n-1} + \alpha_2 x_{n-2} = \epsilon_n, \tag{6}$$

where $\epsilon_n$ is white noise with mean zero. The variance of $\epsilon_n$ is chosen in such a way that the variance of $x_n$ agrees with that of the observed wind data (see Table I).

The parameters $\alpha_i$ of the autoregressive processes are not obtained from the autocorrelation of the first few time lags as standard procedures do (Priestley, 1981), but in an overall sense. They are estimated from the average decay and period of the short time autocorrelation function (see Figure 2a). In this way, we obtained for the $AR(1)$ process $\alpha_1 = -0.9984$ and for the $AR(2)$ process $\alpha_1 = -1.99839$ and $\alpha_2 = 0.998395$. Setting initial values equal to zero, random time series of length $10^7$ are simulated. The results of the dimension analysis is shown in Figure 9. There is no significant difference to the corresponding findings from the observed wind data.

The other type of random noise is constructed by generating a process with similar power spectrum like the observed one but with random phases (Percival and Walden, 1993). The Fourier transform of the phase-randomized signal is constructed by taking the amplitude proportional to the square root of the power spectral density of the observations, and the phases are randomly chosen from a uniform distribution of the interval $(0, 2\pi)$. The time series is obtained by a Fast Fourier backtransform. In order to demonstrate how a phase-randomization influences the estimation of the correlation dimension of a low-dimensional chaotic signal, a time

series of length 20,000 of the Lorenz model (Lorenz, 1963) was generated. The Lorenz model is described by three ordinary differential equations (Lorenz, 1963)

$$\dot{X} = -\sigma X + \sigma Y, \tag{7}$$

$$\dot{Y} = -XZ + rX - Y, \tag{8}$$

$$\dot{Z} = XY - bZ. \tag{9}$$

The parameters are chosen as in Lorenz (1963), namely $\sigma = 10$, $b = 8/3$ and $r = 28$. The numerical integration is performed using a fourth-order Runge Kutta method (Press *et al.*, 1992) and a time step of 0.01. The $X$ variable is taken as a scalar time series stored every 0.25 time units. The power spectrum of the resulting time series follows closely an exponential decay $S(f) \propto \exp(-5.55f)$. The correlation dimension of the original time series and the phase-randomized time series (of length $2^{14}$) are shown in Figure 8. The dimension of the original time series saturates with increasing embedding dimension at the known value of $D_2 = 2.05$ (Grassberger and Procaccia, 1983), whereas the dimension of the phase-randomized signal follows closely the diagonal as is expected for a random signal. Hence, for a system governed by a low-dimensional attractor, the dimensions from the phase-randomized time series clearly deviate from the dimensions obtained from the original time series.

The phase-randomized signal modelling the observed wind data is generated by a power law $f^{-1.54}$ for the power spectral density and random phases as described above. A time series of length $2^{20}$ is obtained by Fast Fourier backtransform. The resulting correlation dimensions for the phase-randomized signals are shown in Figure 9. They also deviate strongly from the diagonal and show a very similar behaviour as the ones of the observations in Figure 6. In contrast to the phase-randomized data from the Lorenz system, the phase-randomization of the wind data does not lead to an increase in the correlation dimension. No difference between the dimensions of the three kinds of random noises in Figure 9 and the measured wind data can be seen. Thus, the time series of observed horizontal wind components can not be distinguished from random noise with the same autocorrelation function. The same dimension calculations are also performed for the absolute value of the horizontal wind vector. Qualitatively the same picture emerges; no sign of a low-dimensional attractor can be detected.

## 5. Conclusions

Fast-response wind measurements were performed in the lower atmospheric boundary layer with an ultrasonic anemometer. The time series of single horizontal wind components as well as of the horizontal wind speed were analyzed with tools developed in the investigations of deterministic chaotic systems. The correlation dimension was estimated by means of a modified Grassberger–Procaccia method.

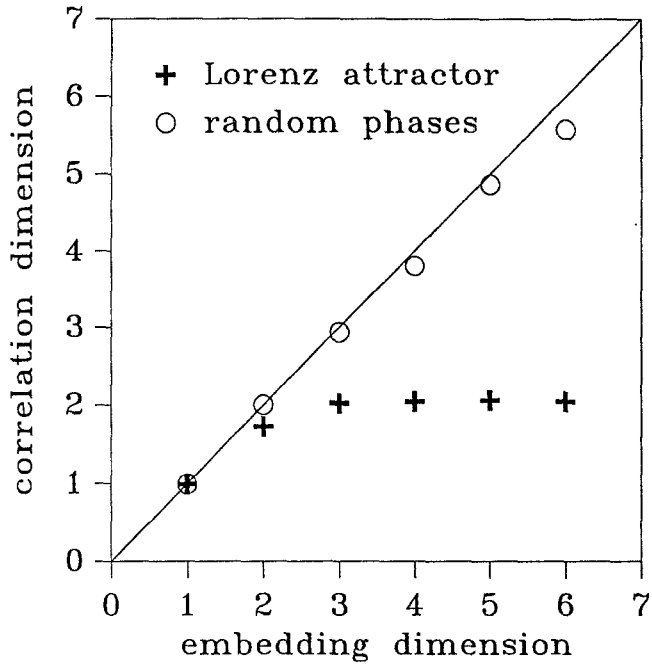


Fig. 8. Correlation dimension of the Lorenz system (crosses) and a phase-randomized signal with similar power spectrum but random phases (circles).

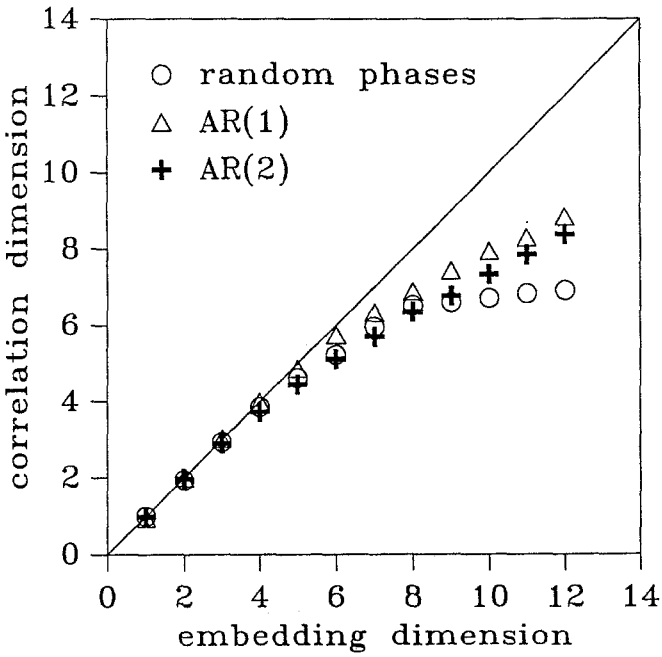


Fig. 9. Same as Figure 6, but for an autoregressive process of first order $AR(1)$ and of second order $AR(2)$, and a random signal with similar spectrum like the observed data but random phases.

The length of the time series allows a reliable estimate of the correlation dimension up to about six, or correspondingly up to an embedding dimension of about thirteen. This is far beyond the limit reached by earlier, shorter data sets as can be seen in Figure 3 of Tsonis *et al.* (1993). No sign of a low-dimensional attractor could be detected within this range. Different types of random signals with similar autocorrelation or similar power spectrum like the observed ones, were numerically generated. A comparison of the dimension estimates from the random time series revealed no differences to the dimensions obtained for the wind data. Therefore, with these methods the wind data can not be distinguished from random noise. Similar negative results for other time series on different time scales were reported in Zeng *et al.* (1992). In Poveda-Jaramillo and Puente (1993) sonic wind data like the ones presented here were investigated and a low-dimensional attractor was found, however, for rather short time series of 18,000 data points. The importance of the amount of required data for the estimation of attractor dimensions has been reviewed in Tsonis *et al.* (1993). In this paper, we emphasized the importance of comparing the natural data with random noise having the same statistical characteristics.

## Acknowledgements

We would like to thank M. Furger and W. Graber for kindly loaning us their anemometer for the measurements and R. Erne and R. Richter for their technical support.

## References

Essex, C., Lookman, T., and Nerenberg, M. A. H.: 1987, 'The Climate Attractor over Short Timescales', *Nature* **326**, 64–66.

Fraedrich, K.: 1986, 'Estimating the Dimensions of Weather and Climate Attractors', *J. Atmos. Sci.* **43**, 419–432.

Grassberger, P.: 1986, 'Do Climatic Attractors Exist?', *Nature* **323**, 609–612.

Grassberger, P. and Procaccia, I.: 1983, 'Characterization of Strange Attractors', *Phys. Rev. Lett.* **50**, 346–349 and 'Measuring the Strangeness of Strange Attractors', *Physica D* **9**, 189–208.

Hentschel, H. G. E. and Procaccia, I.: 1983, 'The Infinite Number of Generalized Dimensions of Fractals and Strange Attractors', *Physica D* **8**, 435–444.

Keppenne, C. L. and Nicolis, C.: 1989, 'Global Properties and Local Structure of the Weather Attractor over Western Europe', *J. Atmos. Sci.* **46**, 2356–2370.

Lorenz, E. N.: 1963, 'Deterministic Nonperiodic Flow', *J. Atmos. Sci.* **20**, 130–141.

Kolmogorov, A. N.: 1941, 'The Local Structure of Turbulence in an Incompressible Viscous Fluid for Very Large Reynolds Numbers', *Dokl. Akad. Nauk SSSR* **30**, 301–305.

Mañé, R.: 1981, 'On the Dimension of the Compact Invariant Sets of Certain Non-Linear Maps', in *Lecture Notes in Mathematics*, Vol. 898, Springer Verlag, New York, pp. 230–242.

Manneville, P.: 1990, *Dissipative Structures and Weak Turbulence*, Academic Press, Boston.

Nerenberg, M. A. H. and Essex, C.: 1990, 'Correlation Dimension and Systematic Geometric Effects', *Phys. Rev. A* **42**, 7065–7074.

Nicolis, C. and Nicolis, G.: 1984, 'Is There a Climatic Attractor?', *Nature* **311**, 529–532.

Percival, D. B. and Walden, A. T.: 1993, *Spectral Analysis for Physical Applications*, Cambridge University Press, Cambridge.

Poveda-Jaramillo, G., and Puente, C. E.: 1993, 'Strange Attractors in Atmospheric Boundary-Layer Turbulence', *Boundary-Layer Meteorol.* **64**, 175–197.

Press, W. H., Teukolsky, S. A., Vetterling, W. T., and Flannery, B. P.: 1992, *Numerical Recipes in Fortran. The Art of Scientific Computing,* Cambridge University Press, Cambridge.

Priestley, M. B.: 1981, *Spectral Analysis of Time Series. Volume 1: Univariate Time Series,* Academic Press, London.

Richardson, L. F.: 1922, *Weather Prediction by Numerical Process,* University Press, Cambridge.

Ruelle, D.: 1990, 'Deterministic Chaos: the Science and the Fiction', *Proc. R. Soc. London A* **427**, 241–248.

Smith, L. A.: 1984, 'Intrinsic Limitations on Dimension Calculations', *Physics Lett. A* **133**, 283–288.

Takens, F.: 1981, 'Detecting Strange Attractors in Turbulence', in *Lecture Notes in Mathematics*, Vol. 898, Springer Verlag, New York, pp. 366–381.

Temam, R.: 1989, *Infinite Dimensional Systems in Mechanics and Physics,* Springer, Berlin.

Theiler, J.: 1986, 'Spurious Dimensions from Correlation Algorithms Applied to Limited Time-Series Data', *Phys. Rev. A* **34**, 2427–2432.

Tsonis, A. A. and Elsner, J. B.: 1988, 'The Weather Attractor over Very Short Time Scales', *Nature* **333**, 545–547.

Tsonis, A. A.: 1992, *Chaos from Theory to Applications,* Plenum Press, New York (1992), pp. 274.

Tsonis, A. A., Elsner, J. B., and Georgakakos, K. P.: 1993, 'Estimating the Dimension of Weather and Climate Attractors: Important Issues about the Procedure and Interpretation', *J. Atmos. Sci.* **50**, 2549–2555.

Zeng, X., Pielke, R. A., and Eykholt, R.: 1992, 'Estimating the Fractal Dimension and the Predictability of the Atmosphere', *J. Atmos. Sci.* **49**, 649–659.